Geophysical Journal International

Geophys. J. Int. (2010) **181,** 1665–1677 doi: 10.1111/j.1365-246X.2010.04583.x

Behaviour of rays at interfaces in anisotropic viscoelastic media

Václav Vavryčuk

Institute of Geophysics, Academy of Sciences, Boční II/1401*, Praha* 4*, Czech Republic. E-mail: vv@ig.cas.cz*

Accepted 2010 February 26. Received 2010 January 5; in original form 2009 May 12

SUMMARY

The behaviour of rays at interfaces in anisotropic viscoelastic media is studied using three different approaches: the real elastic ray theory, the real viscoelastic ray theory and the complex ray theory. In solving the complex eikonal equation, the highest accuracy is achieved by the complex ray theory. The real elastic and viscoelastic ray theories are less accurate but computationally more effective. In all three approaches, the rays obey Snell's law at the interface, but its form is different for each approach. The complex Snell's law constrains the complex tangential components of the slowness vector. The real viscoelastic and elastic Snell's laws constrain the real tangential components of the slowness vector. In the viscoelastic ray theory, the Snell's law is supplemented by the condition of the stationary slowness vector of scattered waves. The accuracy of all three ray theoretical approaches is numerically tested by solving the complex eikonal equation and by calculating the R/T coefficients. The models of the medium consist of attenuating isotropic and anisotropic homogeneous half-spaces with attenuation ranging from extremely strong (Q = 2.5–3) to moderate (Q = 25–30). Numerical modelling shows that solving the complex eikonal equation by the real viscoelastic ray approach is at least 20 times more accurate than solving it by the real elastic ray approach. Also the R/T coefficients are reproduced with a higher accuracy by the real viscoelastic ray approach than by the elastic ray approach.

Keywords: Seismic anisotropy; Seismic attenuation; Wave propagation.

1 INTRODUCTION

Applications of the ray theory to wave propagation problems in anisotropic, inhomogeneous and attenuating media have been intensively studied in recent years (Thomson 1997; Hanyga & Seredyňska 2000; Carcione 2006; Vavryčuk 2007a,b; Červený *et al.* 2008; Vavryčuk 2008a,b). The ray theory yields a high-frequency approximation, which is reasonably accurate in most seismic applications (Červený 2001), and computationally undemanding with respect to other methods solving the equation of motion numerically (Carcione 1990, 1993; Moczo *et al.* 2004, 2007), So far, several ray-theoretical approaches for solving the eikonal equation and modelling of waves in anisotropic attenuating media have been developed. The simplest approach is constructing the rays and other ray quantities in the elastic reference medium and incorporating the effects of attenuation as perturbations (Gajewski & Pšenčík 1992; Vavryčuk 2008b). However, this procedure is applicable to weakly attenuating media only. Alternatively, several authors tried to develop the theory of complex rays (Hearn & Krebes 1990a,b; Le *et al.* 1994; Thomson 1997; Chapman *et al.* 1999; Kravtsov *et al.* 1999; Hanyga & Seredyňska 2000; Kravtsov 2005; Amodei *et al.* 2006). The attenuation is incorporated into the wave modelling by substituting the real-valued elastic parameters by complex-valued and frequency-dependent viscoelastic parameters. Consequently, the eikonal equation and other ray equations become complex and their solution is sought in complex space. The complex ray theory is very accurate in solving the complex eikonal equation, and applicable to anisotropy and attenuation of arbitrary strength. Unfortunately, this theory is computationally complicated and conditioned by successful building of the velocity model in complex space.

Another ray-theoretical approach applicable to solving the complex eikonal equation has been proposed by Vavryčuk (2008a) and called the real viscoelastic ray method. It produces real rays, but all quantities along the rays are complex-valued. The approach is based on the assumption that the complex slowness vector along a ray is stationary and the complex energy velocity vector is homogeneous. The viscoelastic ray approach is less accurate than the complex ray approach, but has proved to be efficient and significantly more accurate than the elastic ray approach.

So far, the viscoelastic ray theory has been developed and all numerical tests have been performed in smoothly inhomogeneous media. In this paper, the theory is completed by deriving formulae for the behaviour of rays at interfaces in anisotropic attenuating media. It is shown that the rays of scattered waves must obey Snell's law, which is similar but not identical with Snell's law in elastic media. The derived theoretical formulae are numerically tested by solving the complex eikonal equation in models of isotropic and anisotropic homogeneous half-spaces with various levels of attenuation. The accuracy of the viscoelastic ray tracing is compared with that produced by real elastic ray tracing and complex ray tracing. The accuracy of the viscoelastic R/T coefficients is also examined.

2 ANISOTROPIC VISCOELASTIC MEDIUM

2.1 Notation

In formulae, the real and imaginary parts of the complex-valued quantities are denoted by superscripts R and I, respectively. A complex-conjugate quantity is denoted by an asterisk. The direction of a complex-valued vector $\mathbf{v}$ is calculated as $\mathbf{v}/\sqrt{\mathbf{v}^T\mathbf{v}}$, where the superscript T means transposition. The magnitude of complex-valued vector $\mathbf{v}$ is complex and is calculated as $\sqrt{\mathbf{v}^T\mathbf{v}}$. If any complex-valued vector is defined by a real-valued direction, it is called homogeneous, and if defined by a complex-valued direction, it is called inhomogeneous.

Besides the standard four-index notation for viscoelastic parameters a_{ijkl} and quality parameters q_{ijkl}, also the two-index Voigt notation A_{MN} and Q_{MN} is used alternatively. The Voigt notation combines pairs of indices i,j or k,l into a single index M or N using the following rules:

$$11 \to 1,\ 22 \to 2,\ 33 \to 3,\ 23 \to 4,\ 13 \to 5,\ 12 \to 6. \tag{1}$$

Quantities in the frequency domain are calculated using the Fourier transform defined as follows:

$$f(\omega) = F\left[f(t)\right] = \int_{-\infty}^{\infty} f(t)\exp(i\omega t)dt. \tag{2}$$

In formulae, the Einstein summation convention is used for repeated subscripts.

2.2 Viscoelastic parameters

A viscoelastic medium is defined by density-normalized viscoelastic parameters a_{ijkl} which are, in general, complex-valued, frequency-dependent and vary with position vector $\mathbf{x}$. The real and imaginary parts of a_{ijkl},

$$a_{ijkl}(\mathbf{x},\omega) = a^R_{ijkl} + i\, a^I_{ijkl}, \tag{3}$$

define elastic and viscous properties of the medium. The ratio between the real and imaginary parts of a_{ijkl} is called the matrix of quality factor parameters,

$$q_{ijkl}(\mathbf{x},\omega) = -\frac{a^R_{ijkl}}{a^I_{ijkl}} \text{ (no summation over repeated indices)}, \tag{4}$$

and quantifies how attenuating the medium is. The sign in eq. (4) depends on the definition of the Fourier transform (2) used for calculating the viscoelastic parameters in the frequency domain. When using the Fourier transform with the exponential term $\exp(-i\omega t)$, the minus sign in (4) must be omitted.

2.3 Complex eikonal equation

The equation of motion for an inhomogeneous anisotropic viscoelastic medium, when no sources are considered, reads [see Červený 2001, eq. (2.1.27)],

$$\rho\omega^2 u_i + (\rho\, a_{ijkl}u_{k,l})_{,j} = 0, \quad i = 1, 2, 3, \tag{5}$$

where $\mathbf{u} = \mathbf{u}(\mathbf{x},\omega)$ is the displacement, $\rho = \rho(\mathbf{x})$ is the density of the medium, $a_{ijkl} = a_{ijkl}(\mathbf{x},\omega)$ are the density-normalized viscoelastic parameters, and ω is the circular frequency. Frequency ω, density ρ and position vector $\mathbf{x}$ are real-valued, viscoelastic parameters a_{ijkl} and displacement $\mathbf{u}$ are complex-valued. Displacement $\mathbf{u} = \mathbf{u}(\mathbf{x},\omega)$ is assumed to describe a high-frequency signal,

$$u_i(\mathbf{x},\omega) = U_i(\mathbf{x})\exp\left[i\omega\tau(\mathbf{x})\right], \tag{6}$$

where $\mathbf{U} = \mathbf{U}(\mathbf{x})$ is the complex-valued amplitude, and $\tau = \tau(\mathbf{x})$ is the complex-valued traveltime. Inserting eq. (6) into the equation of motion (5) and equating terms with ω^2, we obtain the eikonal equation in the form

$$G(\mathbf{x},\mathbf{p}) = a_{ijkl}p_i p_l g_j g_k = 1, \tag{7}$$

where G is the eigenvalue and $\mathbf{g}$ is the normalized complex-valued eigenvector, $\mathbf{g}\cdot\mathbf{g} = 1$, of the Christoffel tensor of the studied wave (P, $S1$ or $S2$)

$$\Gamma_{jk}(\mathbf{x},\mathbf{p}) = a_{ijkl}p_i p_l, \tag{8}$$

and vector $\mathbf{p}$ is the complex-valued slowness vector defined as

$$p_i = \frac{\partial\tau}{\partial x_i}. \tag{9}$$

3 REAL VISCOELASTIC RAY TRACING IN SMOOTHLY INHOMOGENOEUS MEDIA

3.1 Anisotropic media

The eikonal eq. (7) can alternatively be expressed in the following general form [see Červený 2001, eq. (3.6.3)]

$$H(\mathbf{x},\mathbf{p}) = \frac{1}{2}\left(G(\mathbf{x},\mathbf{p}) - 1\right) = 0, \tag{10}$$

where $H = H(\mathbf{x},\mathbf{p})$ is the Hamiltonian. The eikonal equation in the Hamiltonian form (10) represents a non-linear partial differential equation for the complex traveltime $\tau = \tau(\mathbf{x})$. This equation can be solved exactly by using the complex ray tracing equations with complex-valued generalized coordinates $\mathbf{x}$ and $\mathbf{p}$ (see Section 5.1). It can also be solved approximately using the real viscoelastic ray tracing equations with real-valued generalized coordinates $\mathbf{x}$ and $\mathbf{p}^R$ (see Vavryčuk 2008a), where

$$p^R_i = \frac{\partial\tau^R}{\partial x_i}. \tag{11}$$

The inverse quantity to $\mathbf{p}^R$ is the ray velocity $\mathbf{V}^{\mathrm{ray}}$,

$$V^{\mathrm{ray}}_i = \frac{dx_i}{d\tau^R}, \tag{12}$$

which physically means the velocity of a signal propagating along a ray. Eqs (11) and (12) imply the following identity:

$$V^{\mathrm{ray}}_j p^R_j = 1. \tag{13}$$

The real viscoelastic ray tracing equations read

$$\frac{dx_i}{d\tau^R} = \frac{1}{2}\frac{\partial G}{\partial p^R_i}, \quad \frac{dp^R_i}{d\tau^R} = -\frac{1}{2}\frac{\partial G}{\partial x_i}. \tag{14}$$

Substituting (7) into (14) we obtain [see Vavryčuk 2008a, eqs (29), (35) and (A7)]

$$\frac{dx_i}{d\tau^R} = N_i\frac{v^R v^R + v^I v^I}{v^R}, \tag{15}$$

$$\frac{dp_i^R}{d\tau^R} = -\frac{1}{2}\left[\left(\frac{\partial a_{jklm}}{\partial x_i} p_j p_m g_k g_l\right)^R + \frac{v^I}{v^R}\left(\frac{\partial a_{jklm}}{\partial x_i} p_j p_m g_k g_l\right)^I\right], \tag{16}$$

$$\frac{d\tau^I}{d\tau^R} = -\frac{v^I}{v^R}, \tag{17}$$

where energy velocity vector $\mathbf{v}$,

$$v_i = a_{ijkl} p_l g_j g_k, \tag{18}$$

is a complex homogeneous vector and vector $\mathbf{N}$ defines its direction. Since energy velocity vector $\mathbf{v}$ is homogeneous, its real and imaginary parts are parallel. This condition restricts possible values of the complex slowness vector and implies that the real and imaginary parts of the slowness vector are not independent in the ray tracing equations. The slowness vector, which predicts a homogeneous energy velocity vector, is called *stationary* (see Vavryčuk 2007a,b). The stationary slowness vector is, in general, inhomogeneous. The procedure, how to calculate the stationary slowness vector $\mathbf{p}$ is described in Vavryčuk (2008a).

3.2 Isotropic media

The eigenvalue of the Christoffel tensor G in isotropic media reads

$$G(\mathbf{x}, \mathbf{p}^R) = c^2 p_i p_i = 1, \tag{19}$$

where c is the complex-valued phase velocity, $c = \sqrt{(\lambda + 2\mu)/\rho}$ for the P wave and $c = \sqrt{\mu/\rho}$ for the S wave. Parameters λ and μ are complex-valued Lamé's coefficients. Vector $\mathbf{p}$ is the complex-valued slowness vector, $p_i = \partial\tau/\partial x_i$, its magnitude is $p = 1/c$, vector $\mathbf{p}^R$ is its real-valued part, $p_i^R = \partial\tau^R/\partial x_i$ and τ is the complex-valued traveltime. Since the energy velocity vector $\mathbf{v}$,

$$v_i = c^2 p_i. \tag{20}$$

is homogeneous, slowness vector $\mathbf{p}$ must also be homogeneous. This simplifies the ray tracing problem, and the ray tracing equations in anisotropic media (15)–(17) are reduced to the following form in isotropic media [see Vavryčuk 2008a, eqs (39) and (A7)]

$$\frac{dx_i}{d\tau^R} = V^2 p_i^R, \quad \frac{dp_i^R}{d\tau^R} = -\frac{1}{V}\frac{\partial V}{\partial x_i}, \quad \frac{d\tau^I}{d\tau^R} = -\frac{c^I}{c^R}, \tag{21}$$

where V is the real-valued phase velocity calculated from the complex-valued phase velocity c as,

$$V = \frac{1}{\left(c^{-1}\right)^R}, \tag{22}$$

and τ^R is the real part of traveltime τ. Obviously, $V^{\mathrm{ray}} = V$ and $p^R = 1/V^{\mathrm{ray}}$.

4 RAYS AT INTERFACES: REAL VISCOELASTIC APPROACH

4.1 Viscoelastic Snell's law in anisotropic media

Let us assume two homogeneous half-spaces separated by a smoothly curved interface with normal $\mathbf{n}$. This medium can be viewed as a limiting case of a smoothly inhomogeneous medium with a thin transition layer displaying a strong gradient, and the width of the layer shrinking to zero. In this way, we can utilize the ray tracing equations to derive Snell's law. Accordingly, we immediately see that: (1) complex traveltime along a ray is continuous, and (2) the tangential component of vector $\mathbf{p}^R$ is conserved across the interface [see eq. (14)]:

$$\mathbf{p}_\Sigma^R = \mathbf{p}^R - \mathbf{n}(\mathbf{p}^R \cdot \mathbf{n}) = \text{constant}. \tag{23}$$

Since generally three waves are reflected and three waves are transmitted at the interface in anisotropic viscoelastic media, we can express Snell's law in the following form:

$$\mathbf{p}_\Sigma^{(W)R} = \mathbf{p}_\Sigma^{(0)R}, \tag{24}$$

where superscript 0 denotes the incident wave, and superscript $W = 1, \ldots, 6$, denotes the type of scattered wave (P, $S1$ and $S2$ reflected, and P, $S1$ and $S2$ transmitted). Eq. (24) is the real viscoelastic Snell's law. It is emphasized that Snell's law constrains only the real parts of slowness vectors $\mathbf{p}^R$, but not the complete complex-valued slowness vectors $\mathbf{p}$. For elastic media, eq. (24) transforms to the elastic Snell's law.

4.2 Slowness vectors p of scattered waves

The real viscoelastic Snell's law prescribes the value of the tangential component of $\mathbf{p}^R$ at the interface for all scattered waves. The complete complex-valued slowness vector $\mathbf{p}$ must satisfy two conditions. First, it must satisfy the Christoffel equation, and second, it must be stationary. Let us decompose vector $\mathbf{p}$ into its normal and tangential components as follows:

$$\mathbf{p} = \sigma\,\mathbf{n} + \mathbf{p}_\Sigma = \sigma\,\mathbf{n} + \mathbf{p}_\Sigma^R + i\,\mathbf{p}_\Sigma^I, \tag{25}$$

where vector $\mathbf{n}$ is the real-valued normal to interface Σ and σ is the complex-valued scalar. We have to find σ and $\mathbf{p}_\Sigma^I$ for each scattered wave. If we assume that not only $\mathbf{p}_\Sigma^R$, but also $\mathbf{p}_\Sigma^I$ is known, we can calculate σ from the equation for the eigenvalue of the Christoffel tensor Γ_{jk},

$$\det\left(\Gamma_{jk} - \delta_{jk}\right) = 0, \tag{26}$$

which represents an algebraic equation of the 6th degree in σ. Alternatively, we can follow Červený & Pšenčík (2005) and find σ by solving the eigenvalue problem of the 6×6 complex-valued matrix $\mathbf{\Pi}$,

$$\det(\mathbf{\Pi} - \sigma\mathbf{I}_6) = 0, \tag{27}$$

where $\mathbf{I}_m$ denotes the m x m identity matrix and matrix $\mathbf{\Pi}$ is expressed by four 3×3 submatrices,

$$\mathbf{\Pi} = \begin{bmatrix} \mathbf{\Pi}_{11} & \mathbf{\Pi}_{12} \\ \mathbf{\Pi}_{21} & \mathbf{\Pi}_{22} \end{bmatrix}, \tag{28}$$

which are defined as follows

$$\mathbf{\Pi}_{11} = -\left[\mathbf{C}^{(1)}\right]^{-1}\mathbf{C}^{(2)} = \mathbf{\Pi}_{22}^T, \qquad \mathbf{\Pi}_{12} = -\left[\mathbf{C}^{(1)}\right]^{-1},$$
$$\mathbf{\Pi}_{21} = -\mathbf{I}_3 + \mathbf{C}^{(4)} - \mathbf{C}^{(3)}\left[\mathbf{C}^{(1)}\right]^{-1}\mathbf{C}^{(2)}, \quad \mathbf{\Pi}_{22} = -\mathbf{C}^{(3)}\left[\mathbf{C}^{(1)}\right]^{-1}, \tag{29}$$

with

$$C_{ik}^{(1)} = a_{ijkl} n_j n_l, \qquad C_{ik}^{(2)} = a_{ijkl} n_j p_{\Sigma l},$$
$$C_{ik}^{(3)} = a_{ijkl} p_{\Sigma j} n_l, \qquad C_{ik}^{(4)} = a_{ijkl} p_{\Sigma j} p_{\Sigma l}. \tag{30}$$

Calculating σ, we can determine the complete slowness vector $\mathbf{p}$, and subsequently polarization vector $\mathbf{g}$, complex energy velocity vector $\mathbf{v}$, and finally the ray direction $\mathbf{N}$, $\mathbf{N} = \mathbf{v}/v$.

If vector $\mathbf{p}_\Sigma^I$ is chosen arbitrarily, the above procedure will yield a generally complex-valued ray direction $\mathbf{N}$. Since the stationary slowness vector must predict real-valued ray direction $\mathbf{N}$, the procedure must be inverted. The task for the inversion is to find two real-valued components of vector $\mathbf{p}_\Sigma^I$ which yield the real-valued ray direction $\mathbf{N}$. Since the magnitude of vector $\mathbf{p}_\Sigma^I$ is usually small, an inversion with iterations can be applied and several iterations lead to success in most cases.

4.3 Viscoelastic Snell's law in isotropic media

The real viscoelastic Snell's law in isotropic media has the same form as in anisotropic media [see eq. (24)]. However, calculating the complete slowness vectors $\mathbf{p}$ of scattered waves is much simpler in isotropy than in anisotropy. Since the stationary slowness vector is homogeneous (see Section 3.2), vectors $\mathbf{p}^R$ and $\mathbf{p}^I$ are parallel,

$$\mathbf{p} = \mathbf{p}^R + i\mathbf{p}^I = (V^{-1} + iA)\mathbf{N} = V^{-1}(1 + iAV)\mathbf{N}, \tag{31}$$

where $\mathbf{N}$ is the ray direction and A is the ray attenuation (see Vavryčuk 2007b)

$$A = (c^{-1})^I. \tag{32}$$

No inversion problem for calculating $\mathbf{p}^I$ has to be solved. The normal component of vector $\mathbf{p}^R$ is directly obtained as

$$\mathbf{p}_n^R = \pm\sqrt{V^{-2} - \mathbf{p}_\Sigma^R \cdot \mathbf{p}_\Sigma^R}, \tag{33}$$

and the normal and tangential components of $\mathbf{p}^I$ read

$$\mathbf{p}_n^I = AV\mathbf{p}_n^R, \quad \mathbf{p}_\Sigma^I = AV\,\mathbf{p}_\Sigma^R. \tag{34}$$

The sign in eq. (33) is chosen in the same way as in elastic media. For subcritical incidences, the sign discriminates between reflected and transmitted waves. For overcritical incidences, the slowness vector $\mathbf{p}$ of transmitted wave becomes inhomogeneous and the sign of its imaginary normal component must be chosen to satisfy the radiation conditions.

5 RAYS AT INTERFACES: ALTERNATIVE APPROACHES

5.1 Complex Snell's law

The most accurate method for solving the complex eikonal equation is the complex ray theory. In anisotropic smoothly inhomogeneous media, we apply the complex ray tracing equations,

$$\frac{dx_i}{d\tau} = a_{ijkl}p_l g_j g_k, \tag{35}$$

$$\frac{dp_i}{d\tau} = -\frac{1}{2}\frac{\partial a_{jkln}}{\partial x_i}p_k p_n g_j g_l, \tag{36}$$

where all quantities are complex-valued including the ray trajectory $\mathbf{x} = \mathbf{x}(\tau)$. Only the start and endpoints of the ray (i.e. the source and the receiver) lie in real space. This implies that viscoelastic stiffness parameters $a_{ijkl} = a_{ijkl}(\mathbf{x})$ usually considered as functions in real space, must be defined as functions in complex space. Parameters a_{ijkl} can be defined in complex space by analytical continuation of a_{ijkl} from the real to the complex space. However, this procedure is complicated and as yet applicable to simple models only.

At interfaces, we apply the continuity condition of the complex traveltime and the complex Snell's law (Borcherdt 1977, 1982; Wennerberg 1985; Winterstein 1987; Caviglia & Morro 1992; Carcione 2007; Červený 2007)

$$\mathbf{p}_\Sigma^{(W)} = \mathbf{p}_\Sigma^{(0)}, \tag{37}$$

where superscript 0 denotes the incident wave and superscript $W = 1, \ldots, 6$ denotes the type of scattered wave (P, $S1$ and $S2$ reflected, and P, $S1$ and $S2$ transmitted). It is emphasized that the complex Snell's law constrains the real as well as the imaginary parts of the tangential component $\mathbf{p}_\Sigma$ of the slowness vectors, but not just the real part $\mathbf{p}_\Sigma^R$ as assumed in the real viscoelastic Snell's law. The normal components of $\mathbf{p}$ of the scattered waves must be calculated at the interface using the Christoffel equation.

5.2 Elastic Snell's law

A simple approximate method of incorporating attenuation into the ray theory is tracing rays in the elastic reference medium and calculating the effects of attenuation using the first-order perturbations (Gajewski & Pšenčík 1992; Vavryčuk 2008b). The ray tracing equations are identical with those for the elastic reference medium [see Červený 2001, eq. (3.6.10)],

$$\frac{dx_i^R}{d\tau^R} = a_{ijkl}^R p_l^R g_j^R g_k^R, \tag{38}$$

$$\frac{dp_i^R}{d\tau^R} = -\frac{1}{2}\frac{\partial a_{jkln}^R}{\partial x_i^R}p_k^R p_n^R g_j^R g_l^R, \tag{39}$$

where all quantities are real-valued. The ray tracing equations are supplemented by an additional equation for τ^I [see Gajewski & Pšenčík 1992, eq. (10); Vavryčuk 2008b, eq. (59)]

$$\frac{d\tau^I}{d\tau^R} = -\frac{1}{2}a_{ijkl}^I p_i^R p_l^R g_j^R g_k^R. \tag{40}$$

At interfaces, the elastic Snell's law reads,

$$\mathbf{p}_\Sigma^{(W)R} = \mathbf{p}_\Sigma^{(0)R}. \tag{41}$$

The imaginary parts of the slowness vectors $\mathbf{p}$ are identically zero.

The elastic ray approach is approximate and works mostly for weakly attenuating media. Its accuracy can be enhanced by incorporating higher-order perturbations (Klimeš 2002). In several aspects, the elastic and viscoelastic ray approaches are similar. Both approaches solve $\mathbf{x}$, $\mathbf{p}^R$ and τ^I as a function of τ^R and produce real rays. However, the computed ray fields and traveltime $\tau = \tau(\mathbf{x})$ are not identical. The differences are more pronounced in media with strong attenuation. In media with weak attenuation, the differences between both approaches are of the order of the second and higher perturbations.

6 REFLECTION/TRANSMISSION COEFFICIENTS

Having established the Snell's law in viscoelastic media we can readily derive formulae for the viscoelastic ray-theoretical reflection/transmission (R/T) coefficients. The displacement and traction vectors $\mathbf{u}(\mathbf{x}, \omega)$ and $\mathbf{T}(\mathbf{x}, \omega)$ of any of the waves at the interface can be expressed in the following way:

$$\mathbf{u}^{(W)}(\mathbf{x}, \omega) = c^{(W)}\mathbf{g}^{(W)}\exp[i\omega\tau^{(W)}(\mathbf{x})],$$
$$\mathbf{T}^{(W)}(\mathbf{x}, \omega) = c^{(W)}\boldsymbol{\sigma}^{(W)}\exp[i\omega\tau^{(W)}(\mathbf{x})], \tag{42}$$

where $c^{(0)} = 1$ is the unit scalar amplitude of the incident wave, and $c^{(W)}$, $W = 1, \ldots, 6$ is the displacement R/T coefficient of the Wth scattered wave. Vector $\boldsymbol{\sigma}^{(W)}$ is the amplitude-normalized traction vector:

$$\sigma_i^{(W)} = \rho^{(I)} a_{ijkl}^{(I)} n_j g_k^{(W)} p_l^{(W)}. \tag{43}$$

Superscript $I = 1,2$ identifies the half-space, in which the wave propagates. Displacement and traction at the interface must satisfy boundary conditions requiring their continuity across the interface. Since the complex traveltime is continuous along a ray across the interface:

$$\tau^{(0)}(\mathbf{x}) = \tau^{(W)}(\mathbf{x}), \quad W = 1, \ldots, 6, \tag{44}$$

we can omit the common exponential factor $\exp[i\omega\tau^{(W)}(\mathbf{x})]$ in eq. (42) when considering the boundary conditions. If we introduce a 6-vector $\mathbf{d}^{(W)}$ for each wave

$$\mathbf{d}^{(W)} = \pm \begin{bmatrix} \mathbf{g}^{(W)} \\ \boldsymbol{\sigma}^{(W)} \end{bmatrix}, \tag{45}$$

where the plus sign stands for the reflected wave and the minus sign for the transmitted and incident waves, we can express the boundary conditions by the following equation:

$$\mathbf{Dc} = \mathbf{d}^{(0)}. \tag{46}$$

Subsequently, we obtain

$$\mathbf{c} = \mathbf{D}^{-1}\mathbf{d}^{(0)}, \tag{47}$$

where $\mathbf{D}$ is the 6×6 matrix called the displacement-stress matrix, $\mathbf{d}^{(W)}$ is the displacement-stress vector of the Wth wave, and $\mathbf{c}$ is the 6-vector of the displacement R/T coefficients:

$$\mathbf{D} = [\,\mathbf{d}^{(1)} \quad \mathbf{d}^{(2)} \quad \mathbf{d}^{(3)} \quad \mathbf{d}^{(4)} \quad \mathbf{d}^{(5)} \quad \mathbf{d}^{(6)}\,],$$
$$\mathbf{c} = [\,R^P \quad R^{S1} \quad R^{S2} \quad T^P \quad T^{S1} \quad T^{S2}\,]^T. \tag{48}$$

In isotropic media, eq. (47) disintegrates into two separate equations: the first one for the R/T coefficients of the *P-SV* waves, and the second one for the R/T coefficients of the *SH* waves. The both equations can be solved explicitly and their solutions are well known.

The formulae for the ray-theoretical viscoelastic R/T coefficients in isotropic or anisotropic media are formally identical to those valid for the R/T coefficients of the plane waves in viscoelastic isotropic or anisotropic media. The only difference is that the slowness vectors of the incident and scattered waves are calculated in a different way (see Sections 4 and 5). Since the slowness vectors calculated according to the real viscoelastic Snell's law are approximate, the boundary conditions at the interface are satisfied only approximately. Consequently, the viscoelastic R/T coefficients applied to the propagation of plane waves are less accurate than the R/T coefficients calculated using the complex Snell's law. A more accurate result is obtained if the complex traveltime across the interface is calculated according to the viscoelastic Snell's law but the slowness vectors of the scattered waves needed in the formulae for the R/T coefficients are calculated as gradients of the traveltime.

The calculation of the R/T coefficients for overcritical incidences is more involved. The slowness vector of the transmitted wave is no more stationary and the viscoelastic Snell's law must be modified. In this case, the tangential component of the ray direction $\mathbf{N}$ along the interface is real, but the normal component of $\mathbf{N}$ is pure imaginary. The sign of the normal component of $\mathbf{N}$ should be taken in such a way the transmitted wave to satisfy the radiation conditions (Krebes & Daley 2007).

Table 1. Viscoelastic parameters of Models A.

Model	Upper half-space		Lower half-space	
	μ^R/ρ	Q	μ^R/ρ	Q
A1	1.0	5	0.5	2.5
A2	1.0	25	0.5	12.5
A3	1.0	50	0.5	25

Note: μ^R/ρ is in km^2 s^{-2}. Density ρ is 1000 kg m^{-3}.

Table 2. Viscoelastic parameters of Models B.

Model	Upper half-space				Lower half-space			
	a_{44}^R	a_{66}^R	Q_{44}	Q_{66}	a_{44}^R	a_{66}^R	Q_{44}	Q_{66}
B1	1.2	2.4	6	6	0.6	1.2	3	3
B2	1.2	2.4	30	30	0.6	1.2	15	15
B3	1.2	2.4	60	60	0.6	1.2	30	30

Note: a_{44}^R and a_{66}^R are in km^2 s^{-2}. Density ρ is 1000 kg m^{-3}.

7 NUMERICAL EXAMPLES

7.1 Medium model

In this section, the efficiency of the approaches presented above is tested numerically. The model of the medium consists of two homogeneous viscoelastic half-spaces. The half-spaces are in welded contact and the medium density is the same in both half-spaces. Two models are studied: Model A consisting of two isotropic half-spaces and Model B consisting of two transversely isotropic half-spaces with a vertical axis of symmetry. For both models, three levels of attenuation are considered, ranging from extremely strong attenuation with Q of 2.5–3.0 to moderate attenuation with Q of 25–30 (see Tables 1 and 2). The models with the extremely strong attenuation are unrealistic and probably do not reflect any seismic structure.

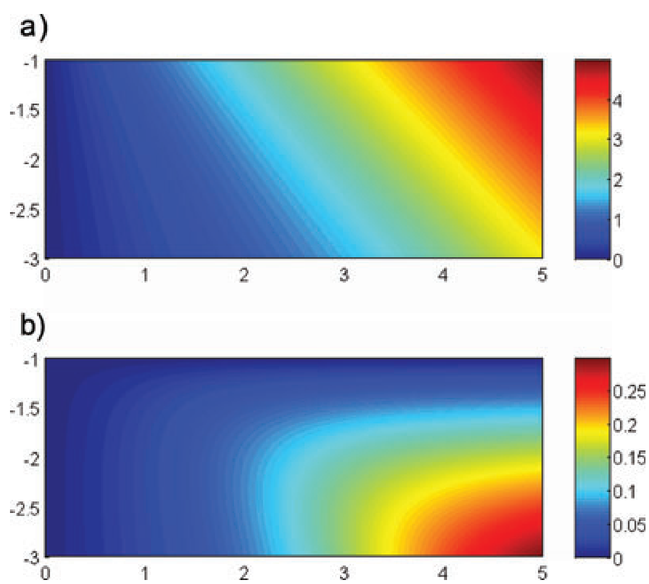

Figure 1. Position of the point of incidence of a complex ray at the interface $x_3 = -1$ for Model A1 as a function of the receiver position in the lower half-space. The real (a) and imaginary (b) parts of the coordinate x_1 of the incidence point at the interface are shown in colours being the function of the receiver position. The colour scale, and the horizontal and vertical scales are in kilometres.

Here they are used to check the robustness of the developed ray methods.

The accuracy of the eikonal equation is studied for the direct and transmitted *SH* waves. The direct wave is generated by the point source situated at the origin of coordinates and lying in the upper half-space. The interface is horizontal at depth $x_3 = -1$ km. The area under study lies in the vertical plane x_1–x_3 being delimited by x_1 between 0 and 5 km and by x_3 between 0 and −3 km. The traveltimes are calculated in a grid with steps of 0.01 km in both horizontal and vertical directions.

The accuracy of the R/T coefficients is studied for plane *SH* waves. The incident wave propagates in the upper half-space. The angle of incidence ranges from 0° to 90° with step of 0.1°. No overcritical incidences appear in the models used. The overcritical incidences are avoided in the numerical modelling because they can cause difficulties in the complex ray theory in selecting a proper sign of the normal component of the slowness vector at the interface (see Krebes & Daley 2007).

7.2 Accuracy of the eikonal equation

7.2.1 *Complex rays*

Since the half-spaces are homogeneous, rays calculated by the complex ray tracing equations (35) and (36) are straight lines. If the source and receiver lie in the same half-space, the rays are straight

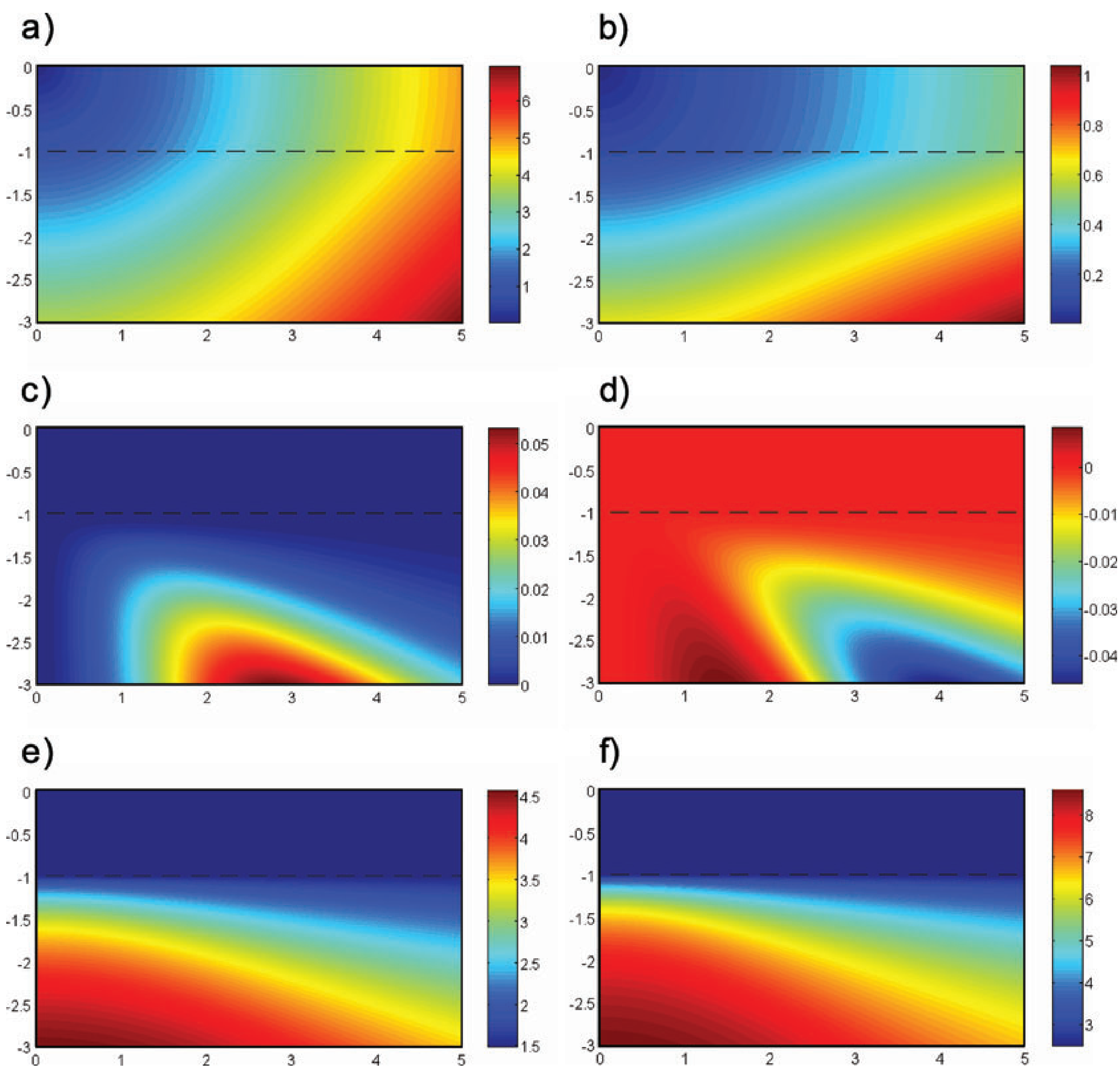

Figure 2. Complex traveltime and its errors in Model A1. (a) Real part of the exact traveltime, τ^R, (b) imaginary part of the exact traveltime, τ^I, (c) errors of τ^R produced by the real viscoelastic ray method, (d) errors of τ^I produced by the real viscoelastic ray method, (e) errors of τ^R produced by the real elastic ray method, (f) errors of τ^I produced by the real elastic ray method. The traveltime (a,b) is in seconds, the errors of the traveltime (c–f) are in per cent. The dashed line shows the interface. The horizontal and vertical scales are in kilometres.

lines in the real space. If the source and receiver lie in different half-spaces, the rays are the piecewise straight lines in the complex space. The complex rays change their directions at the interface according to the complex Snell's law. The geometry of complex rays is calculated according to Appendix A. The slowness vector of a wave outgoing from the source is generally inhomogeneous. For a direct wave, slowness vector **p** is stationary (see Vavryčuk 2007a,b). The energy velocity vector **v** and traveltime τ are calculated using eqs (A2) and (A3), respectively. For a transmitted wave, the slowness vector **p** of the wave outgoing from the source is non-stationary. In Models A, the slowness vector is calculated using eqs (A12) and (A13); in Models B, it is calculated using eqs (A10) and (A11). The complex traveltime is calculated using eq. (A9). The point of incidence of a ray at the interface lies in the complex space having a non-zero imaginary coordinate x_1.

7.2.2 *Real rays*

The real-ray approaches are simpler than the complex-ray approach. The real elastic and viscoelastic rays are calculated using eqs (38–39) and (15–16), respectively. The rays are real straight lines in both half-spaces and change their direction at the interface according to the corresponding Snell's law (elastic or viscoelastic). In the elastic-ray approach, all quantities along a real ray are real-valued except for the traveltime. The imaginary part of the traveltime is calculated using eq. (40). In the viscoelastic-ray approach, the wave

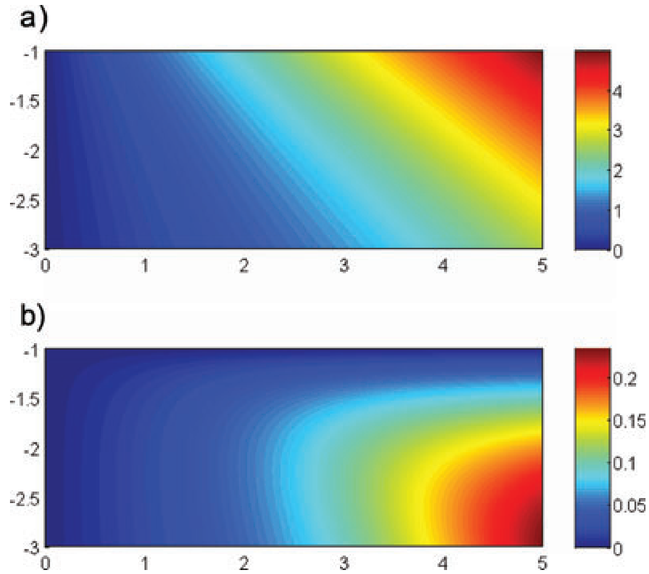

Figure 4. Position of the point of the incidence of a complex ray at the interface $x_3 = -1$ for Model B1 as a function of the receiver position in the lower half-space. The real (a) and imaginary (b) parts of the coordinate x_1 of the incidence point at the interface are shown in colours being the function of the receiver position. The colour scale, and the horizontal and vertical scales are in kilometres.

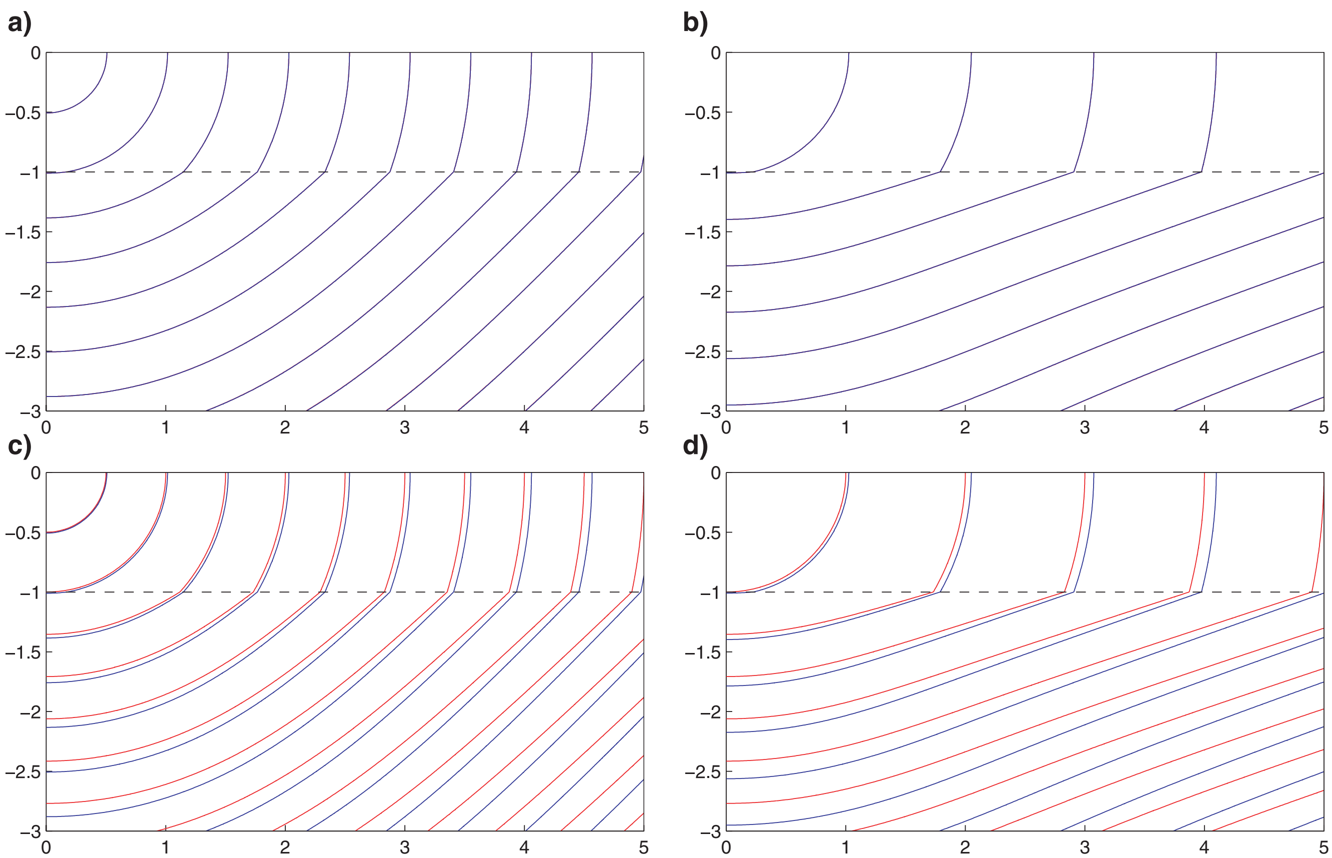

Figure 3. Isochrones in Model A1. Blue line—exact solution calculated using the complex ray theory, red line—approximate solution calculated using the real viscoelastic ray method (a,b), and using the real elastic ray method (c,d). Left-hand plots show the isochrones of the real part of the complex traveltime, right-hand plots show the isochrones of the imaginary part of the complex traveltime. The steps in the real and imaginary isochrones are 0.5 and 0.1s, respectively. The dashed line shows the interface. The vertical and horizontal scales are in kilometres.

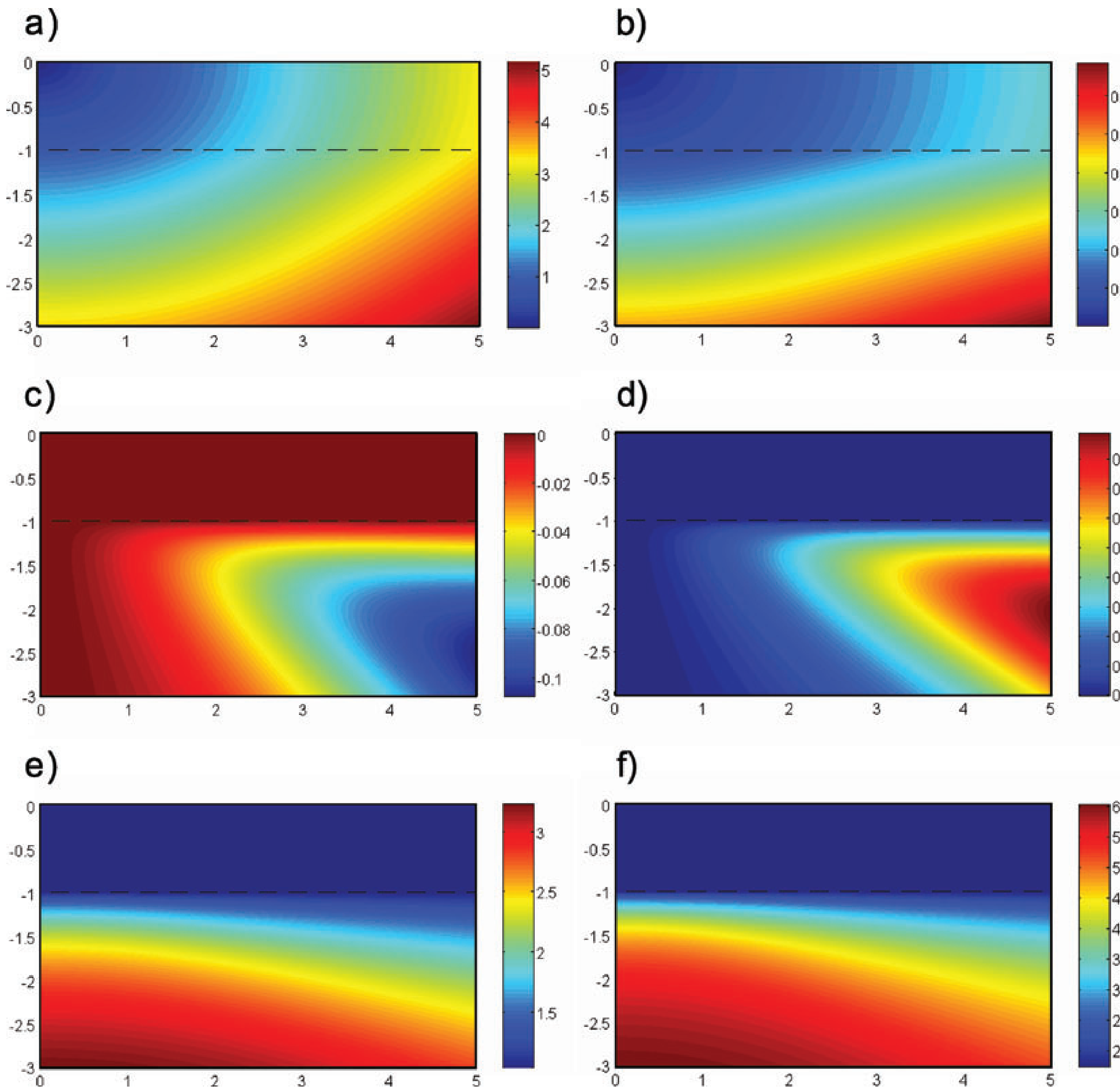

Figure 5. Complex traveltime and its errors in Model B1. (a) Real part of the exact traveltime, τ^R, (b) imaginary part of the exact traveltime, τ^I, (c) errors of τ^R produced by the real viscoelastic ray method, (d) errors of τ^I produced by the real viscoelastic ray method, (e) errors of τ^R produced by the real elastic ray method, (f) errors of τ^I produced by the real elastic ray method. The traveltime (a,b) is in seconds, the errors of the traveltime (c–f) are in per cent. The dashed line shows the interface. The horizontal and vertical scales are in kilometres.

quantities along a real ray are generally complex-valued. The complex slowness vector is inhomogeneous, but the complex energy velocity vector is homogeneous. This applies to the direct as well as transmitted wave. The imaginary part of the traveltime is calculated by applying the quadrature along the ray [see eq. (17)]. For a direct wave, the real viscoelastic-ray approach yields an identical solution with the complex-ray approach. For a transmitted wave, the approaches yield different results.

7.2.3 Comparison of real and complex rays

The most accurate solution of the complex eikonal equation is obtained using complex ray tracing. The crucial step of the complex ray tracing is to find the point of incidence of a complex ray of the transmitted *SH* wave at the interface. The start point of a ray is at the source (at the origin of coordinates), and the endpoint is at the grid of receivers in the lower half-space. The start and endpoints lie in the real space, but the point of incidence of a ray at the interface is in complex space. The positions of the incidence points for the transmitted *SH* wave in Model A1 are shown in Fig. 1. The real and imaginary coordinates of the incidence point vary in dependence on the position of the receiver. For near-vertical incidences the complex rays do not deviate much from the real plane $x_1^R - x_3^R$. However, for shallower incidences and for greater depths of the receivers, the complex rays can deviate significantly from this plane. Obviously, we can expect that, in this area, the approximate real-ray approaches

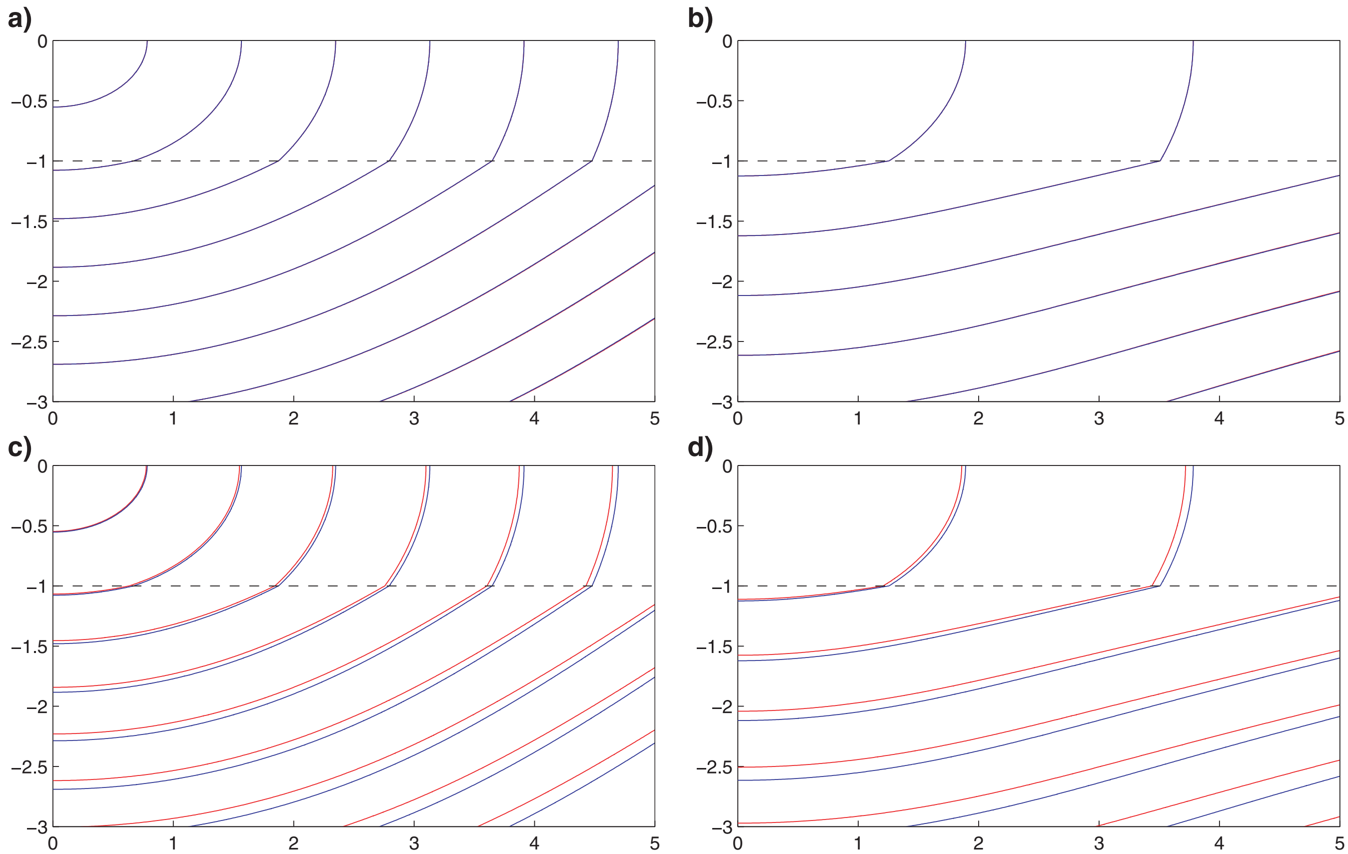

Figure 6. Isochrones in Model B1. Blue line—exact solution calculated using the complex ray theory, red line—approximate solution calculated using the real viscoelastic ray method (a,b), and using the real elastic ray method (c,d). Left-hand plots show the isochrones of the real part of the complex traveltime, right-hand plots show the isochrones of the imaginary part of the complex traveltime. The steps in the real and imaginary isochrones are 0.5 and 0.1 s, respectively. The dashed line shows the interface. The vertical and horizontal scales are in kilometres.

will reproduce the solution of the eikonal equation with the lowest accuracy.

Fig. 2 shows the exact complex traveltime in Model A1 calculated by complex ray tracing (Figs 2a and b) together with errors produced by real viscoelastic ray tracing (Figs 2c and d) and by elastic ray tracing (Figs 2e and f). The errors are calculated at each point of the grid using the following formulae:

$$e_R = \frac{(\tau^{\text{aprox}})^R - (\tau^{\text{exact}})^R}{(\tau^{\text{exact}})^R} 100 \text{ per cent},$$
$$e_I = \frac{(\tau^{\text{aprox}})^I - (\tau^{\text{exact}})^I}{(\tau^{\text{exact}})^I} 100 \text{ per cent}. \quad (49)$$

The maximum errors e_R and e_I of the complex traveltime τ calculated by the real viscoelastic method attain values of up to 5.3×10^{-2} and 4.6×10^{-2} per cent, respectively. The real elastic ray method yields errors of up to 4.6 per cent in τ^R and 8.6 per cent in τ^I. Hence, the accuracy of the viscoelastic ray method is about 100 times higher than that of the elastic ray method. Interestingly, the area of the significant deviation of complex rays from the real plane $x_1^R - x_3^R$ (see Fig. 1) matches the area of low accuracy only very roughly and just for the real viscoelastic rays (see Figs 2c and d). The errors produced by elastic ray tracing display quite a different pattern: the errors mainly reflect inadequate modelling of the traveltime in the extremely attenuating lower half-space ($Q =$ 2.5). This is confirmed in Fig. 3, which shows a comparison of exact and approximate isochrones. The real viscoelastic ray tracing reproduces the isochrones quite well; no differences between the exact and approximate isochrones are observed (see Figs 3a and b). However, the real elastic ray tracing produces isochrones deviating from the exact ones. The deviation is particularly visible at greater depths of the lower half-space (see Figs 3c and d).

Table 3. Errors in the complex traveltime produced by real ray methods.

Model	Elastic rays		Viscoelastic rays	
	e^R (percent)	e^I (percent)	e^R (percent)	e^I (percent)
A1	4.6	8.6	5.3×10^{-2}	4.6×10^{-2}
A2	1.9×10^{-1}	3.5×10^{-1}	2.2×10^{-3}	2.2×10^{-3}
A3	4.8×10^{-2}	8.9×10^{-2}	5.6×10^{-4}	5.6×10^{-4}
B1	3.2	6.0	1.1×10^{-1}	1.8×10^{-1}
B2	1.3×10^{-1}	2.5×10^{-1}	4.6×10^{-3}	7.4×10^{-3}
B3	3.4×10^{-2}	6.2×10^{-2}	1.1×10^{-3}	1.9×10^{-3}

Figs 4–6 display analogous quantities as Figs 1–3, but for Model B1. The results of the numerical modelling for all models are summarized in Table 3. The table shows that the real viscoelastic ray tracing is more accurate than the elastic ray tracing in all models. The accuracy is at least 20 times higher for viscoelastic rays than for elastic rays. As expected, in models with low attenuation, the accuracy of both methods increases.

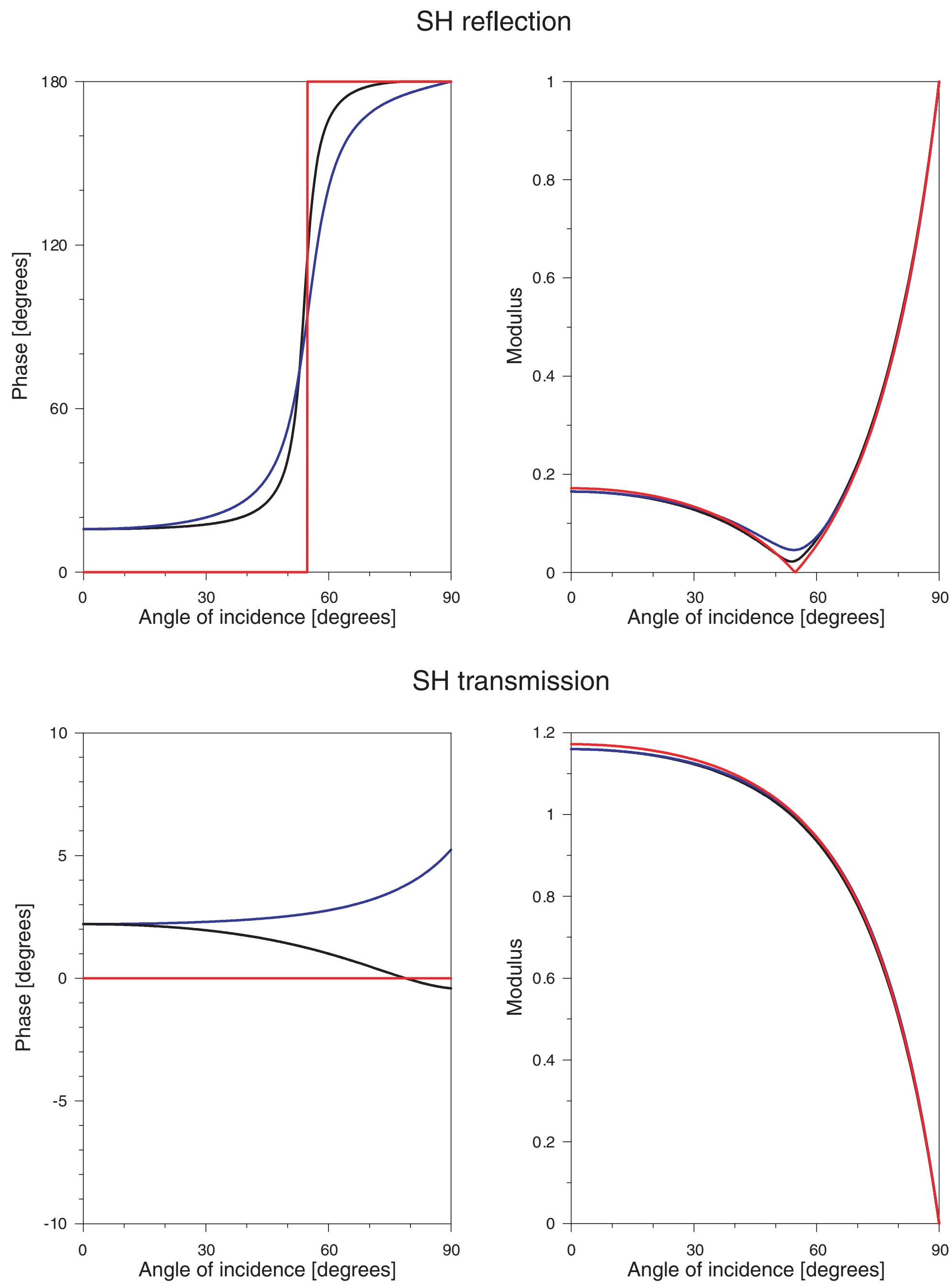

Figure 7. Reflection/transmission coefficients for the plane *SH* waves in model A1. Black line—exact coefficients, blue line—coefficients calculated by the viscoelastic ray approach, red line—elastic coefficients.

7.3 Accuracy of the R/T coefficients

Finally, we examine the accuracy of the R/T coefficients calculated using the viscoelastic ray approach. The viscoelastic R/T coefficients are compared with the exact plane-wave R/T coefficients calculated using the complex Snell's law and with the standard elastic plane-wave R/T coefficients when attenuation is fully neglected.

Fig. 7 shows the phases and moduli of the *SH*-wave R/T coefficients for model A1, which is characterized by extremely strong attenuation. The differences between the three different methods applied are mainly visible in the phase of the reflection coefficient. The phase of the elastic reflection coefficient is zero for incidences between 0° and the Brewster angle (54.7°), and 180° for incidences between the Brewster angle and 90°. At the Brewster angle, the phase is discontinuous. The phase of the real viscoelastic and exact plane-wave reflection coefficients is 15.7° for a normal incidence and gradually increases up to 180° for the incidence of 90°. The phase is smooth having the highest gradient at the Brewster angle. The differences in the phase of the transmission coefficient calculated by the three methods are insignificant being less than 5°. Also the differences in the moduli are almost invisible except for the reflection coefficient in a close vicinity of the Brewster angle.

Fig. 8 shows the phases and moduli of the *SH*-wave R/T coefficients for model A2, which has twice lower attenuation than

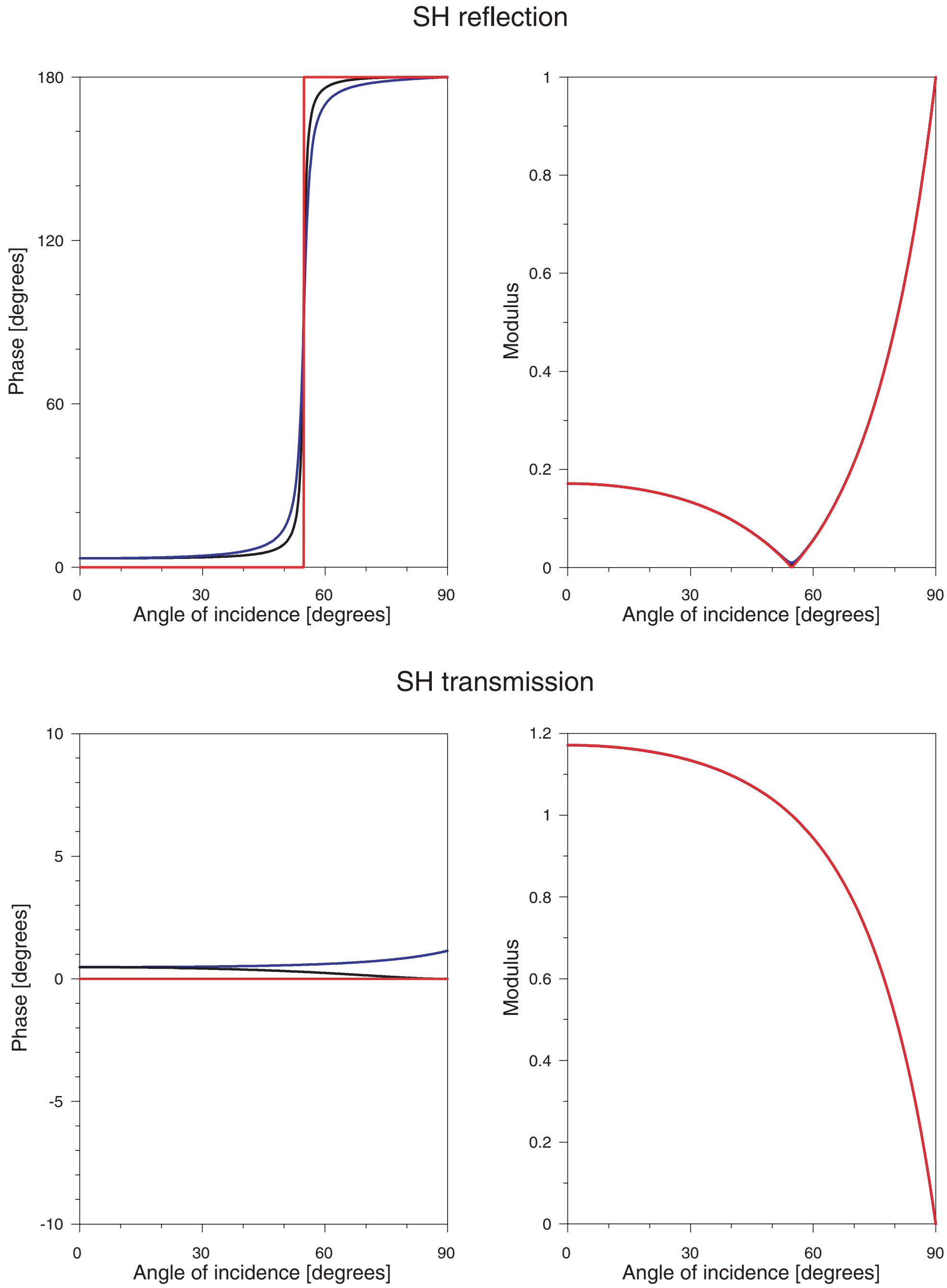

Figure 8. Reflection/transmission coefficients for the plane *SH* waves in model A2. Black line—exact coefficients, blue line—coefficients calculated by the viscoelastic ray approach, red line—elastic coefficients.

model A1. In this case, the differences in the R/T coefficients are practically negligible. The same applies to model A3 characterized by four times lower attenuation than model A1.

The R/T coefficients in models B1–B3 behave in a similar way as in models A1–A3, so they are not shown here.

8 DISCUSSION

The most accurate approach for calculating rays in anisotropic viscoelastic media is the complex ray theory. The rays are calculated using complex ray tracing equations in smoothly inhomogeneous media and obey the complex Snell's law at the interface. The complex Snell's law constrains complex tangential components of slowness vector $\mathbf{p}$. The normal components are calculated using the Christoffel equation. The start and endpoints of a complex ray lie in the real space, but the point of incidence at the interface lies in the complex space.

Less accurate but computationally more efficient approaches are the real viscoelastic and elastic ray methods. The ray tracing equations are simpler and produce real rays. At the interface, the rays obey the real viscoelastic or elastic Snell's law, respectively. The real Snell's laws bind the tangential components of the real part of slowness vectors $\mathbf{p}^R_\Sigma$. All wave quantities along a real ray in the elastic ray approach are real-valued except for the traveltime. The imaginary part of the traveltime is calculated by applying the quadrature along the ray. In the viscoelastic ray approach, the wave quantities along a ray are complex-valued. The complex-valued slowness vector must be stationary. Similarly as in the elastic ray approach, the imaginary part of the traveltime is calculated by applying the quadrature along a ray.

Applying the real viscoelastic Snell's law is more involved than applying the elastic Snell's law. In the elastic ray theory, the slowness vector is real-valued. The elastic Snell's law constrains its tangential components $\mathbf{p}^R_\Sigma$, and the normal components $\mathbf{p}^R_n$ are calculated using the Christoffel equation. The sign of $\mathbf{p}^R_n$ is selected according to the proper ray direction and the radiation conditions. In the viscoelastic ray theory, the slowness vector is complex-valued. The viscoelastic Snell's law constrains the real parts of the tangential components $\mathbf{p}^R_\Sigma$, but not the imaginary parts $\mathbf{p}^I_\Sigma$. Therefore, to determine the complete slowness vector of scattered waves, the other missing components: $\mathbf{p}^R_n$, $\mathbf{p}^I_\Sigma$ and $\mathbf{p}^I_n$, must be calculated. The components $\mathbf{p}^R_n$ and $\mathbf{p}^I_n$ are calculated using the Christoffel equation, the component $\mathbf{p}^I_\Sigma$ can be found using the condition of the stationarity of the slowness vector. However, this computation cannot be done at one step, but by iterations. At this point, the procedure is different from that applied to the complex ray theory. In calculating the complex slowness vector by applying the complex Snell's law, the tangential components of the complete slowness vector $\mathbf{p}_\Sigma$ are conserved. This condition is stronger than that required by the real viscoelastic Snell's law. Consequently, normal component $\mathbf{p}_n$ can be calculated more easily in the complex ray approach, and no procedure with iterations is needed. In isotropic media, the real viscoelastic ray approach simplifies. Since the slowness vector is homogeneous for all scattered waves, no iterations are needed in calculating the missing components of $\mathbf{p}$: $\mathbf{p}^R_n$, $\mathbf{p}^I_\Sigma$ and $\mathbf{p}^I_n$.

Numerical modelling shows that the real viscoelastic ray approach is highly accurate in calculating the traveltimes as well as the R/T coefficients. Isotropic and anisotropic models with various levels of attenuation ranging from extremely strong ($Q = 2.5$–3) to moderate attenuation ($Q = 25$–30) have been used to demonstrate that the real viscoelastic approach is at least 20 times more accurate than the real elastic ray approach when calculating the traveltimes. Also the R/T coefficients are reproduced with a higher accuracy by the real viscoelastic ray approach than by the elastic ray approach.

Numerical modelling also reveals that the accuracy of solving the complex eikonal equation and of calculating the R/T coefficients rapidly increases with decreasing attenuation. In media with Q higher than 100, the differences between the approximate (elastic or viscoelastic) and exact viscoelastic solutions are practically negligible. This implies that the real viscoelastic ray approach can find applications mainly in solving wave propagation problems in rather strongly attenuating media such as in unconsolidated sedimentary rocks. In media with weak attenuation, a simple elastic ray approach considering the attenuation effects as perturbations is fully sufficient. Similarly, if the Q-factor is not extremely variable with frequency then the frequency dependence of the ray fields and the R/T coefficients can be omitted.

ACKNOWLEDGMENTS

I thank Mike Kendall and two anonymous reviewers for their helpful comments. The work was supported by the Grant Agency of the Academy of Sciences of the Czech Republic, Grant No. IAA300120801, and by the Consortium Project 'Seismic Waves in Complex 3-D Structures'.

REFERENCES

Amodei, D., Keers, H., Vasco, W. & Johnson, L., 2006. Computation of uniform wave forms using complex rays, *Phys. Rev. E,* **73**(036704), 1–14.

Borcherdt, R.D., 1977. Reflection and refraction of type-II S waves in elastic and anelastic media, *Bull. seism. Soc. Am.,* **67,** 43–67.

Borcherdt, R.D., 1982. Reflection-refraction of general P- and type-I S waves in elastic and anelastic solids, *Geophys. J. R. astr. Soc.,* **70,** 621–638.

Carcione, J.M., 1990. Wave propagation in anisotropic linear viscoelastic media: theory and simulated wavefields, *Geophys. J. Int.,* **101,** 739–750. Erratum: 1992, **111**, 191.

Carcione, J.M, 1993. Seismic modelling in viscoelastic media, *Geophysics,* **58,** 110–120.

Carcione, J.M., 2006. Vector attenuation: elliptical polarization, raypaths and the Rayleigh-window effect, *Geophys. Prospect.,* **54,** 399–407.

Carcione, J.M., 2007. *Wave Fields in Real Media. Theory and Numerical Simulation of Wave Propagation in Anisotropic, Anelastic, Porous and Electromagnetic Media,* Elsevier Science Publications, Netherlands.

Caviglia, G. & Morro, A., 1992. *Inhomogeneous Waves in Solids and Fluids,* World Scientific, London.

Červený, V., 2001. *Seismic Ray Theory,* Cambridge University Press, Cambridge, UK.

Červený, V., 2007. Reflection/transmission laws for slowness vectors in viscoelastic anisotropic media, *Stud. Geophys. Geod.,* **51,** 391–410.

Červený, V. & Pšenčík, I., 2005. Plane waves in viscoelastic anisotropic media. Part I. Theory, *Geophys. J. Int.,* **161,** 197–212.

Červený, V., Klimeš, L. & Pšenčík, I., 2008. Attenuation vector in heterogeneous, weakly dissipative, anisotropic media, *Geophys. J. Int.,* **175,** 346–355.

Chapman, S.J., Lawry, J.M.H., Ockendon, J.R. & Tew, R.H., 1999. On the theory of complex rays, *SIAM Rev.,* **41,** 417–509.

Gajewski, D. & Pšenčík, I., 1992. Vector wavefield for weakly attenuating anisotropic media by the ray method, *Geophysics,* **57,** 27–38.

Hanyga, A. & Seredyňska, M., 2000. Ray tracing in elastic and viscoelastic media, *Pure appl. Geophys.,* **157,** 679–717.

Hearn, D.J. & Krebes, E.S., 1990a. On computing ray-synthetic seismograms for anelastic media using complex rays, *Geophysics,* **55,** 422–432.

Hearn, D.J. & Krebes, E.S., 1990b. Complex rays applied to wave propagation in a viscoelastic medium, *Pure appl. Geophys.,* **132,** 401–415.

Klimeš, L., 2002. Second-order and higher-order perturbations of travel time in isotropic and anisotropic media, *Stud. Geophys. Geod.,* **46,** 213–248.

Kravtsov, Yu.A., 2005. *Geometrical Optics in Engineering Physics,* Alpha Science, Harrow, UK.

Kravtsov, Yu.A., Forbes, G.W. & Asatryan, A.A., 1999. Theory and applications of complex rays, in *Progress in Optics,* Vol. 39, pp. 3–62, ed. Wolf, E., Elsevier, Amsterdam.

Krebes E.S. & Daley P.F., 2007. Difficulties with computing anelastic plane wave reflection and transmission coefficients, *Geophys. J. Int.,* **170,** 205–216, doi: 10.1111/j.1365-246X.2006.03349.x.

Le, L.H.T., Krebes, E.S. & Quiroga-Goode, G.E., 1994. Synthetic seismograms for *SH* waves in anelastic transversely isotropic media, *Geophys. J. Int.,* **116,** 598–604.

Moczo, P., Kristek, J. & Halada, L., 2004. *The Finite-Difference Method for Seismologists. An Introduction,* 158 pp., Comenius University, Bratislava. ISBN 80-223-2000-5.

Moczo, P., Kristek, J., Gális, M., Pažák, P. & Balazovjech, M., 2007. The finite-difference and finite-element modeling of seismic wave propagation and earthquake motion, *Acta Phys. Slovaca,* **57**(2), 177–406.

Thomson, C.J., 1997. Complex rays and wave packets for decaying signals in inhomogeneous, anisotropic and anelastic media, *Stud. Geophys. Geod.,* **41,** 345–381.

Vavryčuk, V., 2007a. Asymptotic Green's function in homogeneous anisotropic viscoelastic media, *Proc. R. Soc. A,* **463,** 2689–2707, doi: 10.1098/rspa.2007.1862.

Vavryčuk, V., 2007b. Ray velocity and ray attenuation in homogeneous anisotropic viscoelastic media, *Geophysics,* **72**(6), D119–D127, doi: 10.1190/1.2768402.

Vavryčuk, V., 2008a. Real ray tracing in anisotropic viscoelastic media, *Geophys. J. Int.,* **175,** 617–626, doi: 10.1111/j.1365-246X.2008.03898.x.

Vavryčuk, V., 2008b. Velocity, attenuation and quality factor in anisotropic viscoelastic media: a perturbation approach, *Geophysics,* **73**(5), D63–D73, doi: 10.1190/1.2921778.

Wennerberg, L., 1985. Snell's law for viscoelastic materials, *Geophys. J. R. astr. Soc.,* **81,** 13–18.

Winterstein, D.F., 1987. Vector attenuation: some implications for plane waves in anelastic layered media, *Geophysics,* **52**(6), 810–814.

APPENDIX A: COMPLEX RAY TRACING IN A MEDIUM WITH TWO HOMOGENEOUS HALF-SPACES

Let us assume two homogeneous viscoelastic half-spaces separated by a plane horizontal interface at $x_3 = 0$. The source is situated in the upper half-space and the receiver in the lower half-space. Both source and receiver lie in the *x-z* plane. The homogeneous half-spaces defined in the real space are analytically continued to be homogeneous in the complex space. The interface in the complex space is defined by $x_3 = x_3^{\mathrm{R}} + i x_3^I = 0$.

The solution of the complex ray tracing equations (35–36) is elementary in both half-spaces and yields

$$x_i = v_i\,\tau, \tag{A1}$$

where energy velocity vector $\mathbf{v}$,

$$v_i = a_{ijkl} g_j g_k p_l, \tag{A2}$$

and slowness vector $\mathbf{p}$ are constant along the complex ray. If the source and receiver lie in the same half-space, the ray defined as $\mathbf{x} = \mathbf{x}\,(\tau)$ is a straight line in real space. The complex energy velocity vector $\mathbf{v}$ is homogeneous and slowness vector $\mathbf{p}$ is stationary. The stationary slowness vector $\mathbf{p}$ can be calculated using the procedure described in Vavryčuk (2007a,b). The complex traveltime τ is expressed as

$$\tau = \mathbf{p}\cdot\mathbf{x}, \tag{A3}$$

and its real and imaginary parts are related by the following equation:

$$\tau^I = -\frac{v^I}{v^R}\tau^R. \tag{A4}$$

If the source and receiver lie in different half-spaces, the ray consists of two straight line segments. Both segments are, in general, in complex space, only the start and endpoints of the ray lie in real space. If we denote the ray segments in the upper and lower half-spaces by superscripts A and B, respectively,

$$x_1 = x_1^A + x_1^B, \quad x_1^A = \frac{v_1^A}{v_3^A}x_3^A, \quad x_1^B = \frac{v_1^B}{v_3^B}x_3^B, \tag{A5}$$

and taking into account that

$$\tan i^A = \frac{v_1^A}{v_3^A}, \quad \tan i^B = \frac{v_1^B}{v_3^B}, \tag{A6}$$

we obtain

$$x_1 - x_3^A \tan i^A - x_3^B \tan i^B = 0, \tag{A7}$$

where x_1 is the horizontal distance between the source and the receiver, i^A and i^B are angles of a ray at the source and receiver, respectively. Coordinates x_1, x_3^A and x_3^B are real, angles i^A and i^B are complex. The ray angles i^A and i^B are functions of slowness vectors $\mathbf{p}^A$ and $\mathbf{p}^B$ at the source and at the receiver and can be calculated by applying eqs (35) and (A6). The horizontal component of slowness vector $\mathbf{p}^B$ is obtained from $\mathbf{p}^A$ by applying the complex Snell's law at the interface:

$$p_1^A = p_1^B. \tag{A8}$$

The vertical component of $\mathbf{p}^B$ is obtained using the Christoffel equation. Hence, eq. (A7) is actually the equation for the unknown complex take-off angle i_p^A of slowness vector $\mathbf{p}^A$. Having calculated angle i_p^A, and consequently slowness vectors $\mathbf{p}^A$ and $\mathbf{p}^B$, the traveltime comes out as

$$\tau = \tau^A + \tau^B = p_1^A x_1 + p_3^A x_3^A + p_3^B x_3^B. \tag{A9}$$

In transversely isotropic media, eq. (A7) simplifies for the *SH* wave to

$$x_1 - x_3^A \frac{a_{66}^A}{a_{44}^A}\tan i_p^A - x_3^B \frac{a_{66}^B}{a_{44}^B}\tan i_p^B = 0, \tag{A10}$$

where

$$\tan i_p^A = \frac{p_1^A}{p_3^A}, \qquad \tan i_p^B = \frac{p_1^B}{p_3^B} = \frac{p_1^A}{p_3^B}. \tag{A11}$$

In isotropic media, eq. (A7) yields for the *P* or *S* waves

$$x_1 - x_3^A \tan i_p^A - x_3^B \tan i_p^B = 0, \tag{A12}$$

where

$$\tan i_p^A = \frac{p_1^A}{\sqrt{(c^A)^{-2} - (p_1^A)^2}}, \qquad \tan i_p^B = \frac{p_1^A}{\sqrt{(c^B)^{-2} - (p_1^A)^2}}. \tag{A13}$$

Quantities c^A and c^B are the complex phase velocities in the upper and lower half-spaces, respectively.